

A heuristic rule for classification of classical fluids: Master curves for Mie, Yukawa and square-well potentials

Pedro Orea

*Instituto Mexicano del Petróleo, Dirección de Investigación en Transformación de Hidrocarburos,
Eje Central Lázaro Cárdenas 152, 07730 México D.F., Mexico.*

Szabolcs Varga

Institute of Physics and Mechatronics, University of Pannonia, PO Box 158, Veszprém, H-8201 Hungary.

Gerardo Odriozola*

*Área de Física de Procesos Irreversibles, División de Ciencias Básicas e Ingeniería,
Universidad Autónoma Metropolitana, Av. San Pablo 180 Col. Reynosa, 02200 México D.F., Mexico
(Dated: May 12, 2015)*

A shift of the vapor-liquid coexistence curves by the critical value of the reduced second virial coefficient yields striking data collapses to define master curves. This is observed for the Mie, Yukawa and square-well fluids of different attractive ranges. This modification of the extended corresponding-states law of Noro and Frenkel strongly improves the outcomes from the van der Waals principle. Moreover, this shifted extended principle makes the master curves from Mie and Yukawa potentials to be one on top of the other. The square-well potential forms two well defined master curves, each one corresponding to different effective critical exponents.

PACS numbers:

Simple fluids lead to approximately the same compressibility factor when compared at the same reduced temperature and pressure, i. e. all these fluids deviate about the same degree from the ideal behavior. In fact, the van der Waals equation can be written in terms of reduced variables recasting into a substance independent form, when the reduction of variables is made with the corresponding critical values. This invariance can be seen as the principle of corresponding states, stating that two fluids with two equal reduced variables must have the same other reduced properties, and so their states are said to be *corresponding*. This idea was early suggested by van der Waals and 76 years later was proven to be precise for spherically symmetric pairwise additive potentials of the form $A\varphi(r/r_o)$, where r is the interparticle distance and A and r_o are constants [1]. Hence, pairwise additive potentials which produce the same dimensionless $\varphi(x)$ function (of the dimensionless argument x) by rescaling distance and energy must follow the corresponding states principle and are said to be *conformal*. Nowadays, reducing the pair potential with $A = \epsilon$ and $r_o = \sigma$ (being ϵ and σ the energy well depth and distance at which the potential crosses zero, respectively) is a very common and convenient practice when performing computer simulations due to this principle [2].

Letting aside that many body real interactions are never strictly pairwise additive, seldom truly spherically symmetric, and that translational and rotational degrees of freedom may show significant quantization effects, the principle is not expected to work for pair potentials of different attractive ranges [3, 4] (in some cases, however, it does work at the vicinity of the critical point for some potentials of variable range [5–10] and even for bulk structural and dynamical properties when the potential can be written as a sum of exponential functions [11, 12]). This is simply because such potentials are not conformal. This kind of potentials is the rule more than the exception in the colloidal domain, since effective electrostatic and Hamaker interactions are omnipresent and effective polymer-mediated depletion interactions are frequent, contributions showing a strong range dependence on the properties of both phases, dispersed and continuous [13]. With the aim of extending the applicability of the principle to potentials of variable attractive range, at least at the vicinity of the critical point, Noro and Frenkel [14] suggested using the reduced second virial coefficient, B_2^* , as an additional independent variable. Thus, in addition to the σ and ϵ usual quantities to rescale the interparticle potential, they incorporate B_2^* as a measure of its effective attractive range. This was done in view that $B_2^*(T_c^*)$ is almost constant for many different shapes of $\varphi(x)$ functions [15] (being T_c^* the dimensionless critical temperature; we are using the following units: $T^* = k_B T / \epsilon$ for temperature, $\rho^* = \rho \sigma^3$ for density, $r^* = r / \sigma$ for length, and $u^* = u / \epsilon$ for energy). In their proposal $B_2^*(T_c^*) = -1.5$ and so, given a particular $\varphi(x)$, T_c^* is fully determined without the need of a laboratory (or computational) experiment. Moreover, since master curves should exist for all reduced properties when represented against $B_2^*(T^*)$, one would obtain the desired reduced property value for any $\varphi(x)$ and T^* . That is, given $\varphi(x)$, a single variable evaluated at its critical point would be sufficient to predict its

*Electronic address: godriozo@azc.uam.mx

values at other states. This is extremely useful for systems having a difficult to access critical point, such as those governed by strong short-ranged interactions (most colloidal [13] and globular protein suspensions [16, 17]). Nonetheless, the assumption $B_2^*(T_c^*) = cst.$ does not hold when considering from short to intermediate attractive ranges [18–21]. In fact, $B_2^*(T_c^*)$ diverges for the sticky limit of the attractive Yukawa potential [22], which has given rise to propose a modification [22, 23]. Consequently, this assumption leads to imperfect collapses of the reduced properties when represented against $B_2^*(T^*)$ (see figure 13 of reference [17] and the inset at the right panel of figure 1). Note that the direct comparison with the van der Waals corresponding states framework for non conformal potentials is unfair, since in this last case two variables evaluated at the critical point are needed to make it work.

The goal of this work is showing that, for spherically symmetric non conformal potentials from short to intermediate attractive range, the Noro-Frenkel extended framework works better than the original principle for the coexistence densities, when accounting for the fact that, in general, $B_2^*(T_c^*)$ is a function of the attractive range. For this purpose we simply shift the reduced density coexistence curves against B_2^* the quantity $(cst. - B_2^*(T_c^*))$. In other words, we express the reduced densities against $B_{2s}^*(T^*) = B_2^*(T^*) - (B_2^*(T_c^*) - cst.)$, which forces all curves to coincide at the critical point as the van der Waals principle does. This way of comparison between the original and the extended laws turns to be fair. It also makes the extended framework dependent of the critical temperature, though. We are setting $cst. = -1.5$ to gain consistency with previous works [14–17], but probably $cst. = 0$ would be a better choice.

We are mostly taking advantage of the vast data series already published by several authors [10, 24–26] and in previous works [6, 27–29]. We are, however, adding some extra results for the coexistence of the square-well and the attractive Yukawa models at very short attractive ranges, where no data are available. These new data are given in tables at the end of this document. For this purpose we have carried out replica exchange Monte Carlo simulations expanding the isothermal-isocoric ensemble in temperature. Temperatures are set below the critical point and following a geometrical decrease. This way acceptance rates turn similar between two adjacent replicas. The geometrical factor is set to obtain acceptance rates above 10% in all cases (they are close to 20%). We are using rectangular parallelepiped cells with $L_x = L_y = 8.0\sigma$ and $L_z = 40.0\sigma$, while considering a liquid slab at least 10.0σ wide along the z axis. The vapor and liquid phases have similar volumes and their bulk densities are not affected by the presence of the two interfaces. The initial configuration is set close to the vapor-liquid state, by randomly placing N particles within the slab surrounded by vacuum. The center of mass is placed and kept along the simulation run at the cell center. Verlet list are employed to improve performance. After a sufficiently large equilibration time, 10^{10} cycles (consisting on N trial displacements) are considered to obtain the reported densities.

The square well potential reads

$$u^*(r^*) = \begin{cases} \infty, & \text{for } r^* \leq 1, \\ -1, & \text{for } 1 < r^* \leq \lambda, \\ 0, & \text{for } \lambda < r^*, \end{cases} \quad (1)$$

where λ is the range of the attractive well. We obtained new data for $\lambda = 1.10, 1.12, 1.15, 1.20, 1.25, 1.30$ (table V of supplementary materials) and took data for $\lambda = 1.50, 1.75, 2.00, 2.30, 2.50, 2.70$, and 3.0 from elsewhere [25, 26, 29] (tables VI and VII of supplementary materials).

The other two potentials we are considering are the Mie and Yukawa expressions. They are given by

$$u^*(r^*) = \frac{n}{(n-m)} \left(\frac{n}{m} \right)^{\frac{m}{(n-m)}} [(1/r^*)^n - (1/r^*)^m] \quad (2)$$

and

$$u^*(r^*) = \begin{cases} \infty, & \text{for } r^* \leq 1, \\ -\frac{e^{(-\kappa(r^*-1))}}{r^*}, & \text{for } 1 < r^*, \end{cases} \quad (3)$$

respectively. The softness and attractive range for the Mie expression are tuned by n and m , respectively, with $n > m$. We have considered data for $m = 6$ with $n = 8, 10, 12, 18, 20$, and 32 [6, 9] (table I at the end of this document), and also for $n = 2m$ with $m = 7, 9$, and 12 [6] (table II). In the last expression κ defines the attractive range of the Yukawa potential. We are accounting from $\kappa = 3$ to 10 with increments of unity [24, 27, 28], and for $\kappa = 15$ (tables III and IV).

We start the discussion of the results for the Mie and Yukawa potentials. Results for the square-well interaction are given at the end of this work. The reason for doing so is that the shape of the square-well vapor-liquid coexistence curves is nearly cubic for $\lambda \leq 1.75$ and nearly quadratic for $\lambda \geq 2$ [30, 31] when presented as a temperature-density chart. In other words, the effective critical exponent β_c is close to $1/3$ (cubic) or $1/2$ (quadratic) depending on λ . This fact impedes producing a single master curve.

Mie is also known as a generalized Lennard Jones potential since it turns into the Lennard Jones function when setting $n = 12$ and $m = 6$. Furthermore, it allows tuning the hardness of the core-core repulsion (by setting n)

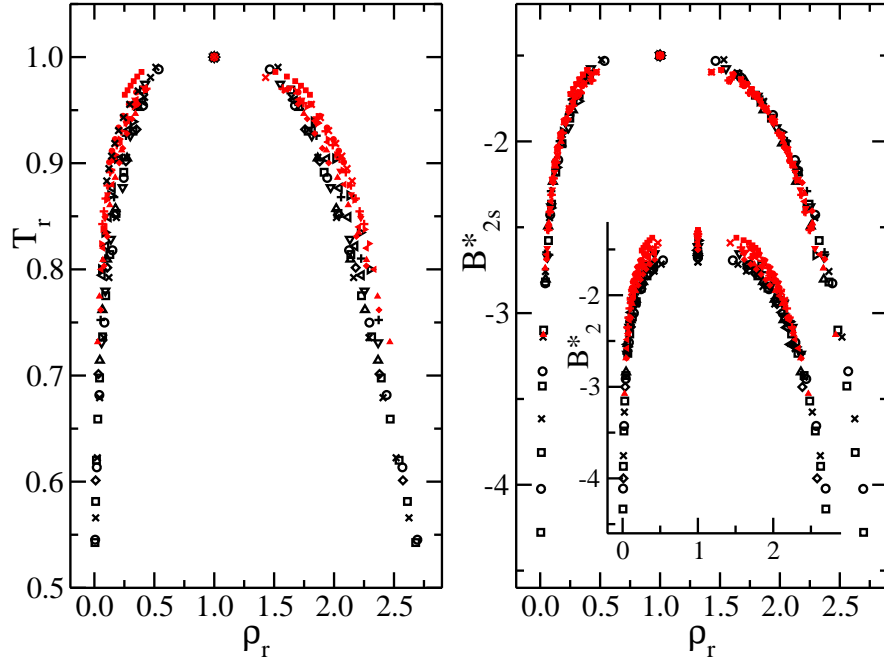


FIG. 1: Vapor-liquid coexistence data for the Mie and Yukawa potentials. Different black open symbols are employed for the Mie potential with different exponents n and m . Different red filled symbols correspond to the attractive Yukawa with different κ . The order of the data as appear in the tables corresponds to squares, circles, diamonds, triangles-up, -left, -down, -right, plus symbols, and crosses in the plots. The corresponding references are also given in the tables. Left) $T_r - \rho_r$ chart as following the van der Waals principle. Right) $B_{2s}^* - \rho_r$ chart. The inset shows the $B_2^* - \rho_r$ chart as following the Noro-Frenkel proposal. The collapse of the data on the right panel is remarkable.

independently of the attractive tail (controlled by m). Thus, Mie presents no discontinuity and so it has not a well defined hard-core diameter. Nonetheless, it is possible to define an effective diameter, σ_{eff} , somewhere in between σ and the distance at which the potential is at its minimum, r_{min} [32]. For this potential we are taking data published by Galliero *et al.* [10] and from previous work [6]. Whenever the critical density and temperature were not available we obtain them by considering $\beta_e = 0.325$ and from the law of rectilinear diameters. All these data and the corresponding B_2^* and B_{2s}^* values are included in tables (see tables at the end of this document). As mentioned, $B_{2s}^*(T^*)$ is simply $B_2^*(T^*) - (B_2^*(T_c^*) - cst.)$ where $B_2^*(T^*) = 3B_2(T^*)/(2\pi\sigma_{eff}^3(T^*))$,

$$B_2(T^*) = 2\pi \int_0^\infty r^{*2} [1 - e^{-u^*(r^*)/T^*}] dr^*, \quad (4)$$

$$\sigma_{eff}^*(T^*) = \int_0^\infty [1 - e^{-u^*(r^*)/T^*}] dr^*, \quad (5)$$

$u^*(r^*) = u^*(r^*) + 1$ for $r^* < r_{min}^*$ and $u'(r^*) = 0$ otherwise [32, 33]. As pointed out above, $1 \leq \sigma_{eff}^* \leq r_{min}^*$. Note that $2\pi\sigma_{eff}^{*3}(T^*)/3$ is the second virial coefficient of hard spheres with $\sigma^* = \sigma_{eff}^*$.

In the left panel of figure 1 the coexistence is given as a $T_r - \rho_r$ chart as following the van der Waals framework. Here $T_r \equiv T^*/T_c^*$ and $\rho_r \equiv \rho^*/\rho_c^*$, being ρ_c^* the critical density. Mie data correspond to black open symbols. As can be seen, there is a relatively good collapse of the data defining a master curve. This finding has been already pointed out by several authors [5, 6, 10]. The data collapse is, however, improved when the coexistence is presented as a $B_{2s}^* - \rho_r$ chart, as following the extended principle proposal and the $B_2^*(T_c^*)$ shift. This is shown in the right panel of the same figure (black open symbols). The shape of this master curve is wider close to the critical point since at this region the relative changes of B_{2s}^* are smaller than that of T_r . Note that the relationship between B_{2s}^* and T^* is not linear, thus the master curve does not fulfill the analogous of a rectilinear diameters law or a scaling law involving the critical exponent β_e . We are also including the $B_2^* - \rho_r$ chart as an inset in the right panel to highlight the strong enhance of the data collapse when accounting for the $B_2^*(T_c^*)$ shift.

Data for the Yukawa fluid are taken from Galicia-Pimentel *et al.* [24] and from previous works [27, 28]. We are also including the case for $\kappa = 15$ from our simulations. Contrasting with the Mie potential, the Yukawa expression

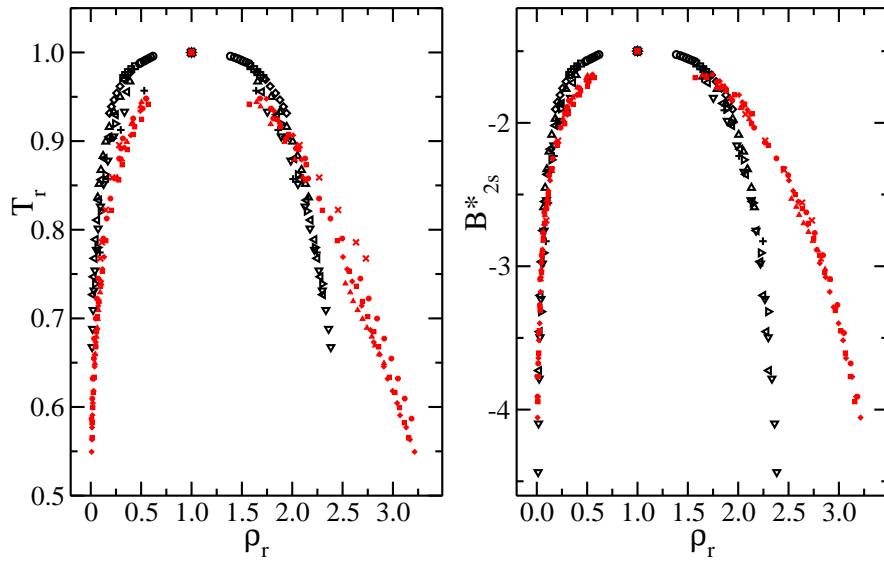


FIG. 2: Vapor-liquid coexistence data for the square-well potential. Different black open symbols are employed for different attractive ranges fulfilling $\lambda \leq 1.75$. Red solid symbols correspond to $\lambda \geq 2.0$. Left) $T_r - \rho_r$ chart as by following the van der Waals principle. Right) $B_{2s}^* - \rho_r$ chart. Data collapse into two different master curves in the right panel.

can only tune its attractive range while having a discontinuity which defines its hard core. Note that in this case $\sigma_{eff} = \sigma = r_{min}$ irrespective of T^* . One would expect this difference to have an effect on the vapor-liquid coexistence, on the possible definition of a master curve, and on its possible shape. Indeed, the data collapse is not so good when the densities are represented in terms of the reduced temperature. This is observed in the left panel of figure 1, where red solid symbols correspond to the Yukawa fluid. Furthermore, the vapor-liquid coexistence gets wider as decreasing the attractive range. Hence, the data are not scattered around a master curve but follow a defined trend. Finally, and as expected, the average curve (not shown) does not coincide with the one obtained for the Mie potential. It is wider close to the critical point and its extrapolation seems to cross the Mie master curve.

A different picture arises when following the extended framework. The result is shown in the right panel of the same figure. Here, not only the data clearly collapse but also the resulting master curve coincides with that obtained for the Mie potential. This allows for a correspondence between different attractive ranges and different potentials types even for not very short attractive ranges (for very short attractive ranges the shape details of the pair potential are expected to lose relevance [14, 34, 35] although this may not be the case [22]). Hence, it is possible the mapping among different potentials by matching B_{2s}^* [14, 17, 36], and to pick a model as a reference system (usually the adhesive hard-sphere potential [37]).

We split the liquid and vapor branches of the master curve to yield an analytic fit. The expression for the liquid branch is given by $B_{2sl}^*(\rho_{rl}) = -0.475(\rho_{rl} - 1)^{3.1} + cst.$, which is strikingly simple. A mirror expression such as $B_{2sv}^*(\rho_{rv}) = -0.563(1 - \rho_{rv})^{3.1} + cst.$ can only match the vapor branch close to the critical point. We have found that $B_{2sv}^*(\rho_{rv}) = -(a\rho_{rv}^3 + b\rho_{rv}^{0.5})^{-1} + (a + b)^{-1} + cst.$ with $a = 75.1$ and $b = 3.71$ fits its general shape. Note that a single computational experiment for $T^* < T_c^*$ to obtain ρ_l^* and ρ_v^* is enough to determine the whole binodal by using these expressions. That is, by equating $B_{2sl}^*(\rho_l^*/\rho_c^*)$ and $B_{2sv}^*(\rho_v^*/\rho_c^*)$ one gets ρ_c^* . Then from $B_{2sl}^*(\rho_l^*/\rho_c^*) = B_{2s}^*(T_c^*)$, T_c^* is obtained. With this knowledge (and function $u^*(r^*)$) the complete binodal can be built. It will be interesting to test the predictions for other $u^*(r^*)$ functions.

The square-well potential can be seen as a special case. Although it is considered the simplest model capable of producing a vapor-liquid coexistence, its corresponding fluid behavior is far from simple. The energy flatness of the well and the second discontinuity at $r^* = \lambda$ lead to a peculiar radial distribution function for the liquid phase [38], which in turn is translated to all thermodynamic bulk properties. Moreover, it shows an oscillatory behavior for the critical density with λ [39, 40] and a steep change in the shape of the coexistence curve when transiting from $\lambda = 1.75$ to $\lambda = 2.0$ [30, 31]. This change is probably related to the fact that only the first coordination shell contributes to the total potential energy for $\lambda \leq 1.75$ and a second contributing shell appears at some point in between these two values [41]. Hence, the short attractive range suddenly turns into a not so short range, producing a jump of the effective critical exponent from $\beta_e \sim 0.325$ to $\beta_e \sim 0.5$. In other words, the nearly cubic shape of the coexistence shift to something nearly quadratic. This fact had raised questions on its belonging to the 3D Ising universality class [30, 31]. In addition, $B_2^*(T_c^*)$ also oscillates when plotted against λ , producing values significantly different from

−1.5 (see references [18–20] and tables).

Figure 2 shows the vapor-liquid coexistence for the square-well in terms of T_r and B_{2s}^* in the left and right panels, respectively. Here, we are presenting new coexistence data for very short attractive range cases ($\lambda \leq 1.3$). Critical values well agree with those obtained from a mapping procedure of the grand canonical density distribution onto the universal Ising model distribution [21]. For cases having $\lambda \geq 1.5$, data were taken from previous work [29], from del Río *et al.* [25], and from Patel *et al.* [26]. We are employing the effective exponents $\beta_e = 0.325$ and $\beta_e = 0.5$ for $\lambda \leq 1.75$ and $\lambda \geq 2.0$, respectively, to obtain the critical parameters (all these data are given in tables). The short range results ($\lambda \leq 1.75$) are given as black open symbols and red solid symbols are used for $\lambda \geq 2.0$. Short attractive range results seem to collapse when plotted against T_r , whereas results for $\lambda \geq 2.0$ produce wider coexistences as increasing λ . Nonetheless, the collapse for $\lambda \leq 1.75$ is clearly improved when using B_{2s}^* . Moreover, the results for $\lambda \geq 2.0$ do also yield a master curve when plotted against B_{2s}^* . In this case we are not including the $B_2^* - \rho_r$ chart since $B_2^*(T_c^*)$ depends more strongly on the attractive range and so, the data collapse is poor. Unfortunately, the short range master curve for the square-well does not lie above the one found for Mie and Yukawa. The vapor branch is very similar, though (the same expression with $a = 74.3$ and $b = 3.3$ produces a good match). The liquid do not match the simple shape $a(\rho_{rl} - 1)^b + cst$.

In brief, we have compared the outcomes from the original van der Waals framework with those from a slight modification of the Noro-Frenkel proposal for non conformal potentials of variable attractive range. This has been done for short and intermediate attractive ranges, but for the vapor-liquid coexistence only. Results indicate that the extended framework works better than the original principle, once the corresponding shift of $B_2^*(T_c^*)$ from the proposed value is accounted for. This is pointed out, at least, for the Mie, Yukawa, and square-well potentials. Moreover, it is shown how the Mie and Yukawa potentials yield the same master curve. For the square-well case, two well defined master curves were obtained. It remains an open question how many master curves exist for simple fluids interacting for spherically symmetric pair potentials. In this work we have detected only three curves, but it may happen that new ones arise for some special shapes or ranges of the attractive interaction. It is also questionable whether the shifted extended principle of the phase coexistence can be extended for patchy colloids [42] or liquid crystals where the interaction is anisotropic.

I. ACKNOWLEDGEMENTS

PO thank the Instituto Mexicano del Petróleo for financial support (Project No D.60019). GO thanks CONACyT Project No 169125.

-
- [1] K. E. Pitzer, J. Chem. Phys. **7**, 583 (1939).
 - [2] D. Frenkel and B. Smit, *Understanding molecular simulation* (Academic, New York, 1996).
 - [3] E. A. Guggenheim, J. Chem. Phys. **13**, 253 (1945).
 - [4] T. W. Leland and P. S. Chapple, Ind. Eng. Chem. **60**, 15 (1968).
 - [5] H. Okumura and F. Yonezawa, J. Chem. Phys. **113**, 9162 (2000).
 - [6] P. Orea, Y. Reyes-Mercado, and Y. Duda, Phys. Lett. A **372**, 7024 (2008).
 - [7] D. O. Dunikov, S. P. Malysenko, and V. V. Zhakhovskii, J. Chem. Phys. **115**, 6623 (2001).
 - [8] V. C. Weiss and W. Schröer, Int. J. Thermophys. **28**, 506 (2007).
 - [9] P. Grosfils and J. F. Lutsko, J. Chem. Phys. **130**, 054703 (2009).
 - [10] G. Galliero, M. M. Piñeiro, B. Mendiboure, C. Miqueu, T. Lafitte, and D. Bessieres, J. Chem. Phys. **130**, 104704 (2009).
 - [11] J. Dyre, Phys. Rev. E. **87**, 022106 (2013).
 - [12] A. Bacher, T. B. Schröder, and J. Dyre, Nat. Commun. **5**, 5424 (2014).
 - [13] R. J. Hunter, *Foundations of Colloid Science* (Oxford University Press, Oxford, 2001), 2nd ed.
 - [14] M. G. Noro and D. Frenkel, J. Chem. Phys. **113**, 2941 (2000).
 - [15] G. A. Vliegenthart and H. N. W. Lekkerkerker, J. Chem. Phys. **112**, 5364 (2000).
 - [16] P. Katsonis, S. Brandon, and P. G. Vekilov, J. Phys. Chem. B **110**, 17638 (2006).
 - [17] N. E. Valadez-Pérez, A. L. Benavides, E. Schöll-Paschinger, and R. Castañeda-Priego, J. Chem. Phys. **137**, 084905 (2012).
 - [18] D. Fu, Y. Li, and J. Wu, Phys. Rev. E. **68**, 011403 (2003).
 - [19] R. López-Rendón, Y. Reyes, and P. Orea, J. Chem. Phys. **125**, 084508 (2006).
 - [20] S. Zhou, Mol. Sim. **33**, 1187 (2007).
 - [21] J. Largo, M. A. Miller, and F. Sciortino, J. Chem. Phys. **128**, 134513 (2008).
 - [22] D. Gazzillo and D. Pini, J. Chem. Phys. **139**, 164501 (2013).
 - [23] E. Schöll-Paschinger, N. E. Valadez-Pérez, A. L. Benavides, and R. Castañeda-Priego, J. Chem. Phys. **139**, 184902 (2013).

- [24] U. F. Galicia-Pimentel, J. López-Lemus, and P. Orea, *Fluid Phase Equilib.* **265**, 205 (2008).
- [25] F. del Río, E. Ávalos, R. Espíndola, L. F. Rull, G. Jackson, and S. Lago, *Mol. Phys.* **100**, 2531 (2002).
- [26] B. H. Patel, H. Docherty, S. Varga, A. Galindo, and G. C. Maitland, *Mol. Phys.* **103**, 129 (2005).
- [27] Y. Duda, A. Romero-Martínez, and P. Orea, *J. Chem. Phys.* **126**, 224510 (2007).
- [28] G. Odriozola, M. Barcenas, and P. Orea, *J. Chem. Phys.* **134**, 154702 (2011).
- [29] P. Orea, Y. Duda, V. C. Weiss, W. Schröer, and J. Alejandre, *J. Chem. Phys.* **120**, 11754 (2004).
- [30] L. Vega, E. de Miguel, L. F. Rull, G. Jackson, and I. A. McLure, *J. Chem. Phys.* **96**, 2296 (1992).
- [31] E. de Miguel, *Phys. Rev. E* **55**, 1347 (1997).
- [32] J. A. Barker and D. Henderson, *Rev. Mod. Phys.* **48**, 587 (1976).
- [33] H. C. Andersen, J. D. Weeks, and D. Chandler, *Phys. Rev. A* **4**, 1597 (1971).
- [34] G. Foffi, C. D. Michele, F. Sciortino, and P. Tartaglia, *Phys. Rev. Lett.* **94**, 078301 (2005).
- [35] G. Foffi and F. Sciortino, *Phys. Rev. E* **74**, 050401(R) (2006).
- [36] A. González-Calderón and A. Rocha-Ichante, *J. Chem. Phys.* **142**, 034305 (2015).
- [37] R. J. Baxter, *J. Chem. Phys.* **49**, 2770 (1968).
- [38] J. Largo, J. R. Solana, S. B. Yuste, and A. Santos, *J. Chem. Phys.* **122**, 084510 (2005).
- [39] A. Gil-Villegas, F. del Río, and A. L. Benavides, *Fluid Phase Equilib.* **119**, 97 (1996).
- [40] E. Schöll-Paschinger, A. L. Benavides, and R. Castañeda-Priego, *J. Chem. Phys.* **123**, 234513 (2005).
- [41] Y. Reyes-Mercado, C. A. Flores-Sandoval, and P. Orea, *J. Chem. Phys.* **139**, 164505 (2013).
- [42] G. Foffi and F. Sciortino, *J. Phys. Chem. B* **111**, 9702 (2007).

TABLE I: Coexistence properties and second virial coefficients for Mie fluids as a function of parameters n and m . These cases correspond to $m = 6$ with $n = 8, 10, 12, 18, 20$, and 32 . See the article for symbol definitions.

$n - m$	T^*	ρ_L^*	ρ_V^*	B_2	B_2^*	B_{2s}
8-6 ^a	1.000	0.811	0.0034	-8.332	-3.752	-3.616
	1.100	0.778	0.008	-7.180	-3.276	-3.140
	1.200	0.744	0.014	-6.266	-2.894	-2.758
	1.300	0.708	0.024	-5.523	-2.581	-2.444
	1.400	0.669	0.038	-4.908	-2.319	-2.182
	1.500	0.624	0.057	-4.391	-2.096	-1.959
	1.600	0.576	0.083	-3.950	-1.904	-1.768
	1.700	0.508	0.129	-3.570	-1.737	-1.600
	1.750	0.473	0.159	-3.399	-1.661	-1.525
critical point	1.767	0.309	0.309	-3.343	-1.636	-1.500
10-6 ^a	0.800	0.825	0.0021	-9.307	-4.112	-4.024
	0.900	0.786	0.006	-7.653	-3.427	-3.339
	1.000	0.746	0.013	-6.427	-2.914	-2.827
	1.100	0.702	0.026	-5.484	-2.516	-2.428
	1.200	0.650	0.046	-4.736	-2.196	-2.108
	1.300	0.594	0.075	-4.129	-1.934	-1.847
	1.400	0.512	0.124	-3.627	-1.715	-1.628
	1.450	0.448	0.164	-3.407	-1.619	-1.531
critical point	1.467	0.306	0.306	-3.336	-1.588	-1.500
12-6 ^a	0.700	0.842	0.0015	-9.865	-4.334	-4.277
	0.750	0.820	0.003	-8.746	-3.869	-3.812
	0.800	0.798	0.006	-7.821	-3.482	-3.425
	0.850	0.775	0.009	-7.044	-3.156	-3.099
	0.900	0.752	0.014	-6.382	-2.876	-2.819
	0.950	0.726	0.022	-5.812	-2.634	-2.577
	1.000	0.699	0.030	-5.316	-2.423	-2.366
	1.050	0.672	0.041	-4.880	-2.236	-2.179
	1.100	0.638	0.057	-4.495	-2.070	-2.013
	1.150	0.602	0.077	-4.152	-1.922	-1.865
	1.200	0.560	0.101	-3.845	-1.788	-1.731
	1.250	0.515	0.129	-3.568	-1.667	-1.610
critical point	1.300	0.312	0.312	-3.318	-1.557	-1.500
18-6 ^b	0.750	0.781	0.015	-6.310	-2.839	-2.803
	0.800	0.745	0.022	-5.595	-2.530	-2.494
	0.850	0.705	0.035	-4.995	-2.269	-2.234
	0.900	0.666	0.058	-4.483	-2.046	-2.011
	0.950	0.615	0.090	-4.042	-1.853	-1.818
	1.000	0.565	0.122	-3.658	-1.684	-1.649
critical point	1.050	0.330	0.330	-3.321	-1.535	-1.500
20-6 ^a	0.750	0.772	0.020	-5.852	-2.643	-2.674
	0.800	0.735	0.030	-5.177	-2.349	-2.380
	0.850	0.695	0.045	-4.610	-2.101	-2.132
	0.900	0.643	0.077	-4.127	-1.889	-1.920
	0.950	0.591	0.098	-3.710	-1.706	-1.736
	1.000	0.505	0.138	-3.348	-1.545	-1.576
critical point	1.026	0.326	0.326	-3.177	-1.469	-1.500
32-6 ^b	0.650	0.809	0.018	-5.798	-2.638	-2.646
	0.700	0.759	0.031	-4.996	-2.282	-2.290
	0.750	0.702	0.056	-4.343	-1.991	-1.999
	0.800	0.632	0.090	-3.802	-1.749	-1.757
	0.825	0.581	0.124	-3.564	-1.642	-1.650
critical point	0.864	0.340	0.340	-3.231	-1.492	-1.500

^aData taken from J. Chem. Phys. **130**, 104704 (2009)

^bData taken from Phys. Lett. A **372**, 7024 (2008)

TABLE II: Coexistence properties and second virial coefficients for Mie fluids as a function of parameters n and m (continued from TABLE I). These cases correspond to $n = 2m$ with $m = 7, 9$, and 12 . See the article for symbol definitions.

$n - m$	T^*	ρ_L^*	ρ_V^*	B_2	B_2^*	B_{2s}
14-7 ^b	0.600	0.842	0.0035	-9.109	-4.000	-3.952
	0.700	0.778	0.011	-6.751	-3.002	-2.954
	0.800	0.713	0.035	-5.215	-2.346	-2.298
	0.850	0.668	0.056	-4.634	-2.096	-2.047
	0.900	0.615	0.086	-4.140	-1.882	-1.834
	0.930	0.575	0.115	-3.878	-1.768	-1.720
critical point	0.996	0.330	0.330	-3.360	-1.548	-1.500
18-9 ^b	0.580	0.802	0.024	-5.683	2.537	-2.527
	0.600	0.783	0.035	-5.260	2.353	-2.343
	0.620	0.762	0.042	-4.879	2.188	-2.178
	0.640	0.736	0.054	-4.536	2.038	-2.028
	0.660	0.698	0.076	-4.225	1.902	-1.892
	0.680	0.655	0.104	-3.941	1.778	-1.768
	0.700	0.601	0.145	-3.682	1.664	-1.654
critical point	0.730	0.360	0.360	-3.332	1.510	-1.500
24-12 ^b	0.460	0.897	0.023	-5.706	-2.564	-2.662
	0.480	0.865	0.034	-5.086	-2.290	-2.388
	0.500	0.831	0.053	-4.553	-2.054	-2.152
	0.520	0.785	0.075	-4.091	-1.848	-1.946
	0.540	0.715	0.125	-3.686	-1.668	-1.766
critical point	0.575	0.390	0.390	-3.089	-1.402	-1.500

^bData taken from Phys. Lett. A **372**, 7024 (2008)

TABLE III: Coexistence properties and second virial coefficients for attractive Yukawa fluids with different κ . See the article for symbol definitions.

κ	T^*	ρ_L^*	ρ_V^*	B_2	B_2^*	B_{2s}
3.0 ^c	0.550	0.847	0.0187	-5.631	-2.688	-2.686
	0.580	0.809	0.029	-5.042	-2.407	-2.405
	0.600	0.780	0.038	-4.697	-2.242	-2.240
	0.650	0.698	0.074	-3.963	-1.892	-1.890
	0.660	0.679	0.085	-3.835	-1.830	-1.829
	0.670	0.656	0.097	-3.711	-1.772	-1.770
	0.680	0.633	0.112	-3.594	-1.716	-1.714
	0.690	0.607	0.129	-3.480	-1.661	-1.660
	0.700	0.576	0.152	-3.371	-1.609	-1.608
critical point	0.722	0.357	0.357	-3.146	-1.502	-1.500
4.0 ^d	0.425	0.937	0.010	-6.440	-3.075	-3.126
	0.450	0.898	0.016	-5.628	-2.687	-2.738
	0.470	0.863	0.027	-5.078	-2.425	-2.476
	0.485	0.838	0.035	-4.714	-2.251	-2.302
	0.500	0.805	0.049	-4.384	-2.093	-2.144
	0.515	0.771	0.066	-4.084	-1.950	-2.001
	0.530	0.736	0.086	-3.810	-1.819	-1.870
	0.550	0.664	0.130	-3.480	-1.661	-1.712
	0.581	0.380	0.380	-3.034	-1.448	-1.500
5.0 ^d	0.400	0.932	0.0227	-5.403	-2.580	-2.659
	0.410	0.906	0.029	-5.065	-2.418	-2.498
	0.420	0.880	0.036	-4.755	-2.270	-2.350
	0.440	0.832	0.059	-4.207	-2.009	-2.087
	0.460	0.776	0.087	-3.737	-1.784	-1.863
	0.470	0.734	0.111	-3.527	-1.684	-1.763
	0.480	0.680	0.140	-3.330	-1.590	-1.669
	0.485	0.640	0.170	-3.237	-1.546	-1.625
	0.500	0.399	0.399	-2.976	-1.421	-1.500
6.0 ^d	0.380	0.925	0.037	-4.730	-2.258	-2.361
	0.390	0.892	0.046	-4.392	-2.097	-2.199
	0.400	0.852	0.060	-4.084	-1.950	-2.053
	0.420	0.770	0.110	-3.545	-1.693	-1.795
	0.430	0.720	0.140	-3.308	-1.579	-1.682
	0.435	0.680	0.170	-3.197	-1.526	-1.629
	0.448	0.416	0.416	-2.927	-1.398	-1.500
7.0 ^e	0.340	0.988	0.025	-5.202	-2.483	-2.622
	0.346	0.972	0.030	-4.952	-2.365	-2.503
	0.351	0.955	0.036	-4.715	-2.251	-2.390
	0.357	0.935	0.043	-4.488	-2.143	-2.282
	0.363	0.917	0.052	-4.272	-2.040	-2.178
	0.369	0.893	0.063	-4.066	-1.941	-2.080
	0.375	0.870	0.076	-3.868	-1.847	-1.986
	0.381	0.839	0.092	-3.679	-1.756	-1.895
	0.387	0.806	0.113	-3.498	-1.670	-1.809
	0.394	0.764	0.142	-3.325	-1.588	-1.726
	0.400	0.685	0.183	-3.159	-1.508	-1.647
critical point	0.413	0.431	0.431	-2.850	-1.361	-1.500

^cData taken from Fluid Phase Equilib. **265**, 205 (2008)

^dData taken from J. Chem. Phys. **126**, 224510 (2007)

^eData taken from J. Chem. Phys. **134**, 154702 (2011)

TABLE IV: Coexistence properties and second virial coefficients for attractive Yukawa fluids with different κ (continued from TABLE III). See the article for symbol definitions.

κ	T^*	ρ_L^*	ρ_V^*	B_2	B_2^*	B_{2s}
8.0 ^e	0.325	0.997	0.030	-4.919	-2.349	-2.516
	0.330	0.980	0.036	-4.700	-2.244	-2.411
	0.335	0.966	0.042	-4.491	-2.144	-2.311
	0.339	0.948	0.049	-4.290	-2.048	-2.215
	0.344	0.929	0.058	-4.098	-1.956	-2.123
	0.349	0.906	0.069	-3.913	-1.868	-2.035
	0.354	0.881	0.083	-3.736	-1.783	-1.950
	0.359	0.855	0.100	-3.566	-1.702	-1.869
	0.364	0.822	0.121	-3.403	-1.624	-1.792
	0.369	0.772	0.150	-3.246	-1.550	-1.717
critical point	0.375	0.696	0.192	-3.095	-1.478	-1.645
	0.387	0.443	0.443	-2.791	-1.332	-1.500
9.0 ^e	0.321	0.976	0.047	-4.308	-2.057	-2.225
	0.325	0.957	0.055	-4.120	-1.967	-2.135
	0.330	0.937	0.065	-3.939	-1.880	-2.049
	0.334	0.914	0.078	-3.765	-1.798	-1.966
	0.338	0.887	0.092	-3.598	-1.718	-1.886
	0.343	0.856	0.110	-3.437	-1.641	-1.809
	0.347	0.822	0.134	-3.282	-1.567	-1.736
	0.352	0.767	0.166	-3.134	-1.496	-1.665
	0.357	0.648	0.213	-2.991	-1.428	-1.596
	0.364	0.454	0.454	-2.789	-1.331	-1.500
critical point	0.313	0.967	0.058	-4.024	-1.921	-2.113
	0.316	0.948	0.068	-3.857	-1.841	-2.033
	0.320	0.928	0.080	-3.696	-1.765	-1.956
	0.324	0.902	0.094	-3.541	-1.691	-1.882
	0.328	0.876	0.112	-3.392	-1.619	-1.811
	0.332	0.840	0.135	-3.249	-1.551	-1.743
	0.336	0.790	0.163	-3.110	-1.485	-1.677
	0.348	0.465	0.465	-2.740	-1.308	-1.500
critical point	0.313	0.967	0.058	-4.024	-1.921	-2.113
	0.316	0.948	0.068	-3.857	-1.841	-2.033
	0.320	0.928	0.080	-3.696	-1.765	-1.956
	0.324	0.902	0.094	-3.541	-1.691	-1.882
	0.328	0.876	0.112	-3.392	-1.619	-1.811
	0.332	0.840	0.135	-3.249	-1.551	-1.743
	0.336	0.790	0.163	-3.110	-1.485	-1.677
	0.348	0.465	0.465	-2.740	-1.308	-1.500
critical point	0.2822	0.902	0.128	-3.167	-1.512	-1.724
	0.2834	0.885	0.139	-3.106	-1.483	-1.695
	0.2847	0.865	0.152	-3.046	-1.454	-1.666
	0.2859	0.841	0.165	-2.988	-1.426	-1.638
	0.2872	0.806	0.179	-2.930	-1.399	-1.611
	0.2885	0.758	0.198	-2.873	-1.372	-1.584
	0.2926	0.502	0.502	-2.697	-1.288	-1.500
	0.2822	0.902	0.128	-3.167	-1.512	-1.724
	0.2834	0.885	0.139	-3.106	-1.483	-1.695
	0.2847	0.865	0.152	-3.046	-1.454	-1.666

^eData taken from J. Chem. Phys. **134**, 154702 (2011)

^fThis work

TABLE V: Coexistence properties and second virial coefficients for square-well fluids with different λ . See the article for symbol definitions.

λ	T^*	ρ_L^*	ρ_V^*	B_2	B_2^*	B_{2s}
1.10 ^f	0.4710	0.747	0.230	-3.006	-1.435	-1.573
	0.4717	0.733	0.238	-2.988	-1.427	-1.564
	0.4726	0.719	0.252	-2.971	-1.419	-1.556
	0.4730	0.707	0.261	-2.954	-1.410	-1.548
	0.4737	0.693	0.272	-2.937	-1.402	-1.540
	0.4743	0.677	0.283	-2.920	-1.394	-1.532
	0.4750	0.659	0.293	-2.903	-1.386	-1.524
critical point	0.4770	0.476	0.476	-2.853	-1.362	-1.500
1.12 ^f	0.5021	0.806	0.151	-3.272	-1.562	-1.665
	0.5038	0.791	0.160	-3.229	-1.542	-1.645
	0.5055	0.777	0.173	-3.188	-1.522	-1.626
	0.5073	0.762	0.189	-3.147	-1.503	-1.606
	0.5090	0.745	0.206	-3.106	-1.483	-1.586
critical point	0.5170	0.470	0.470	-2.925	-1.397	-1.500
1.15 ^f	0.536	0.863	0.082	-3.873	-1.849	-1.905
	0.540	0.849	0.091	-3.768	-1.799	-1.855
	0.544	0.834	0.103	-3.666	-1.751	-1.806
	0.549	0.814	0.114	-3.566	-1.703	-1.759
	0.553	0.791	0.129	-3.469	-1.656	-1.712
	0.558	0.770	0.148	-3.373	-1.611	-1.666
	0.562	0.732	0.174	-3.280	-1.566	-1.622
critical point	0.575	0.444	0.444	-3.025	-1.444	-1.500
1.20 ^f	0.562	0.903	0.029	-5.414	-2.585	-2.589
	0.572	0.890	0.035	-5.129	-2.449	-2.453
	0.583	0.874	0.042	-4.859	-2.320	-2.324
	0.594	0.858	0.051	-4.601	-2.197	-2.201
	0.604	0.837	0.062	-4.355	-2.079	-2.083
	0.616	0.813	0.077	-4.121	-1.968	-1.972
	0.627	0.784	0.096	-3.898	-1.861	-1.865
	0.638	0.748	0.121	-3.685	-1.760	-1.764
	0.650	0.692	0.162	-3.482	-1.663	-1.667
critical point	0.672	0.418	0.418	-3.133	-1.496	-1.500
1.25 ^f	0.557	0.910	0.008	-7.940	-3.791	-3.728
	0.572	0.900	0.011	-7.371	-3.519	-3.456
	0.588	0.888	0.014	-6.842	-3.267	-3.204
	0.604	0.877	0.019	-6.352	-3.033	-2.969
	0.621	0.862	0.024	-5.896	-2.815	-2.752
	0.638	0.846	0.032	-5.471	-2.612	-2.549
	0.656	0.820	0.041	-5.075	-2.423	-2.360
	0.674	0.797	0.054	-4.705	-2.247	-2.183
	0.693	0.766	0.073	-4.360	-2.082	-2.018
	0.712	0.730	0.098	-4.037	-1.928	-1.864
	0.732	0.671	0.142	-3.735	-1.783	-1.720
critical point	0.766	0.395	0.395	-3.374	-1.563	-1.500
1.30 ^f	0.579	0.882	0.005	-9.483	-4.528	-4.436
	0.597	0.874	0.007	-8.772	-4.188	-4.097
	0.616	0.864	0.009	-8.117	-3.875	-3.784
	0.635	0.850	0.012	-7.512	-3.587	-3.495
	0.654	0.838	0.015	-6.953	-3.320	-3.228
	0.675	0.822	0.021	-6.435	-3.073	-2.981
	0.696	0.805	0.027	-5.955	-2.843	-2.752
	0.717	0.787	0.035	-5.509	-2.631	-2.539
	0.739	0.761	0.047	-5.095	-2.433	-2.342
	0.762	0.735	0.063	-4.710	-2.249	-2.157
	0.786	0.700	0.084	-4.350	-2.077	-1.986
critical point	0.810	0.649	0.124	-4.015	-1.917	-1.826
critical point	0.868	0.370	0.370	-3.333	-1.591	-1.500

^fThis work

TABLE VI: Coexistence properties and second virial coefficients for square-well fluids with different λ (continued from TABLE V). See the article for symbol definitions.

λ	T^*	ρ_L^*	ρ_V^*	B_2	B_2^*	B_{2s}
1.50 ^g	0.900	0.693	0.013	-8.042	-3.840	-3.317
	0.950	0.671	0.020	-7.183	-3.430	-2.907
	1.000	0.647	0.030	-6.453	-3.081	-2.558
	1.050	0.620	0.044	-5.824	-2.781	-2.258
	1.100	0.586	0.063	-5.278	-2.520	-1.997
	1.120	0.570	0.073	-5.079	-2.425	-1.902
critical point	1.218	0.302	0.302	-4.237	-2.023	-1.500
1.75 ^h	1.400	0.595	0.024	-7.426	-3.546	-2.826
	1.550	0.532	0.045	-6.180	-2.951	-2.231
	1.650	0.493	0.079	-5.513	-2.632	-1.912
	1.730	0.435	0.109	-5.050	-2.411	-1.691
critical point	1.808	0.265	0.265	-4.649	-2.220	-1.500
2.00 ^g	2.100	0.642	0.024	-6.848	-3.270	-2.681
	2.150	0.619	0.028	-6.588	-3.145	-2.557
	2.250	0.577	0.038	-6.110	-2.917	-2.329
	2.350	0.533	0.054	-5.682	-2.713	-2.124
	2.450	0.487	0.072	-5.295	-2.528	-1.940
critical point	2.736	0.235	0.235	-4.374	-2.089	-1.500
2.30 ⁱ	2.60	0.847	0.002	-8.876	-4.238	-3.910
	2.70	0.829	0.004	-8.390	-4.006	-3.678
	2.80	0.811	0.005	-7.945	-3.793	-3.465
	2.90	0.794	0.008	-7.536	-3.598	-3.270
	3.00	0.775	0.009	-7.158	-3.418	-3.090
	3.10	0.756	0.013	-6.809	-3.251	-2.923
	3.20	0.734	0.016	-6.485	-3.096	-2.769
	3.30	0.712	0.020	-6.184	-2.953	-2.625
	3.50	0.664	0.033	-5.640	-2.693	-2.365
	3.60	0.633	0.042	-5.394	-2.576	-2.248
	3.70	0.603	0.052	-5.163	-2.465	-2.137
	3.80	0.574	0.063	-4.946	-2.362	-2.034
	3.90	0.566	0.075	-4.742	-2.264	-1.936
	3.95	0.542	0.080	-4.644	-2.217	-1.889
	4.00	0.516	0.085	-4.548	-2.172	-1.844
	4.10	0.482	0.112	-4.366	-2.085	-1.757
	4.15	0.476	0.137	-4.278	-2.043	-1.715
	4.20	0.447	0.146	-4.193	-2.002	-1.674
critical point	4.43	0.266	0.266	-3.828	-1.828	-1.500
2.50 ⁱ	3.30	0.783	0.003	-8.747	-4.177	-3.945
	3.40	0.772	0.003	-8.379	-4.001	-3.769
	3.50	0.760	0.005	-8.035	-3.837	-3.605
	3.60	0.749	0.006	-7.713	-3.683	-3.451
	3.70	0.735	0.008	-7.411	-3.538	-3.307
	3.90	0.709	0.012	-6.858	-3.275	-3.043
	4.00	0.697	0.013	-6.605	-3.154	-2.922
	4.10	0.682	0.016	-6.366	-3.040	-2.808
	4.20	0.669	0.020	-6.140	-2.932	-2.700
	4.30	0.654	0.024	-5.925	-2.829	-2.598
	4.40	0.636	0.028	-5.722	-2.732	-2.500
	4.60	0.607	0.037	-5.344	-2.551	-2.320
	4.80	0.570	0.051	-5.000	-2.387	-2.156
	5.00	0.529	0.069	-4.687	-2.238	-2.007
	5.10	0.530	0.077	-4.541	-2.168	-1.937
	5.20	0.512	0.090	-4.401	-2.101	-1.870
	5.30	0.487	0.105	-4.266	-2.037	-1.805
	5.35	0.466	0.108	-4.201	-2.006	-1.774
	5.40	0.459	0.125	-4.137	-1.975	-1.744
	5.50	0.390	0.141	-4.013	-1.916	-1.685
critical point	5.84	0.248	0.248	-3.626	-1.731	-1.500

^gData taken from J. Chem. Phys. **120**, 11754 (2004)

^hData taken from Mol. Phys. **100**, 2531 (2002)

ⁱData taken from Mol. Phys. **103**, 129 (2005)

TABLE VII: Coexistence properties and second virial coefficients for square-well fluids with different λ (continued from TABLE VI). See the article for symbol definitions.

λ	T^*	ρ_L^*	ρ_V^*	B_2	B_2^*	B_{2s}
2.70 ⁱ	4.00	0.778	0.002	-9.019	-4.306	-4.055
	4.10	0.767	0.003	-8.714	-4.161	-3.910
	4.20	0.758	0.003	-8.425	-4.023	-3.772
	4.30	0.743	0.004	-8.151	-3.892	-3.641
	4.40	0.736	0.005	-7.890	-3.767	-3.516
	4.50	0.725	0.007	-7.643	-3.649	-3.398
	4.60	0.713	0.008	-7.407	-3.537	-3.286
	4.70	0.704	0.009	-7.183	-3.430	-3.179
	4.80	0.694	0.010	-6.969	-3.327	-3.076
	4.90	0.680	0.012	-6.764	-3.230	-2.979
	5.00	0.672	0.014	-6.569	-3.136	-2.886
	5.20	0.651	0.018	-6.203	-2.962	-2.711
	5.40	0.628	0.025	-5.866	-2.801	-2.550
	5.50	0.616	0.028	-5.708	-2.725	-2.474
	5.60	0.606	0.032	-5.556	-2.653	-2.402
	6.40	0.506	0.071	-4.523	-2.160	-1.909
	6.50	0.494	0.081	-4.413	-2.107	-1.856
	6.60	0.486	0.096	-4.307	-2.056	-1.806
	6.70	0.454	0.100	-4.204	-2.007	-1.756
	6.80	0.440	0.119	-4.105	-2.960	-1.709
	6.90	0.422	0.134	-4.008	-2.914	-1.663
critical point	7.28	0.242	0.242	-3.667	-1.751	-1.500
3.00 ⁱ	6.50	0.722	0.010	-6.962	-3.324	-3.093
	6.60	0.710	0.011	-6.814	-3.253	-3.022
	6.70	0.700	0.012	-6.671	-3.185	-2.954
	6.80	0.692	0.014	-6.532	-3.119	-2.887
	6.90	0.680	0.016	-6.398	-3.055	-2.823
	7.00	0.669	0.017	-6.268	-2.993	-2.761
	7.10	0.657	0.019	-6.142	-2.932	-2.701
	7.20	0.646	0.020	-6.019	-2.874	-2.642
	7.30	0.639	0.023	-5.900	-2.817	-2.586
	7.40	0.627	0.026	-5.785	-2.762	-2.530
	8.60	0.523	0.065	-4.620	-2.206	-1.974
	8.80	0.502	0.077	-4.459	-2.129	-1.897
	9.00	0.477	0.089	-4.305	-2.055	-1.824
	9.20	0.443	0.100	-4.158	-1.985	-1.754
	9.40	0.418	0.122	-4.018	-1.918	-1.687
	9.45	0.408	0.125	-3.984	-1.902	-1.671
critical point	10.01	0.248	0.248	-3.627	-1.732	-1.500

ⁱData taken from Mol. Phys. **103**, 129 (2005)